A Flexible Planar Antenna on Multilayer Rubber Composite for Wearable Devices

Abdullah Al-Sehemi[1, 2]**, Ahmed Al-Ghamdi**[3]**, Nikolay Dishovsky**[4]**,
Gabriela Atanasova**[5, 6]**, and Nikolay Atanasov**[5, 6, *]

Abstract—This paper presents the design of a flexible antenna using planar dipole with a reflector to achieve optimal radiation efficiency and low specific absorption rate (SAR) when the antenna is placed directly over the skin of body model. The antenna is designed for the 2.45 GHz frequency band. The parametric analysis of the proposed antenna is carried out. The proposed antenna achieves stable on-body performance: $|S_{11}|$ varies from -16.05 dB (on skin) at 2.47 GHz resonant frequency to -16.40 dB (in free space) at 2.44 GHz resonant frequency. It was found that the maximum 1 g average SAR value is only 0.23 W/kg for an input power of 100 mW when the antenna is placed directly over the skin of a three-layer body model, and radiation efficiency is 20.5%. The measured results are presented to demonstrate the validity of the proposed antenna.

1. INTRODUCTION

Wearable devices have become one of the fastest growing consumer segments of the Internet of Things [1]. They can be used in many different consumer sectors such as sports, personal safety, medical, and lifestyle computing.

Wearable devices, in essence, are wireless devices equipped with antenna, sensors, processor and operating system as well as user-friendly interface and can be embedded in clothing or accessories. As one of the key components in the communication system, wearable antennas have received much attention in both academia and industry since their unconventional operating environment is in extremely close proximity to the human body [2].

Designing antenna for wearable devices has several critical challenges. One of the most challenging aspects of designing wearable antennas is avoiding, as much as possible, the negative effect of interaction between the antenna and the dissipative biological tissue [3]. The proximity of user's head or body to the wireless device has several consequences, such as modification of the antenna radiation pattern, input impedance variation, and detuning of the resonant frequency [4]. Simultaneously, the impact of a wearable antenna on human tissue, characterized by the specific absorption rate (SAR), also needs to be minimized [2]. Furthermore, wearable antennas have to have light weight, high flexibility, low profile, low cost and simple structure for easy fabrication.

In literature, researchers have worked on both reduction of SAR values in the human tissue of a wearable antenna and reduction of detuning effects from human body on the antenna performance. Different design approaches have been proposed: (i) using metasurfaces [5], including electromagnetic band-gap structures [6], (ii) using artificial magnetic conducting surfaces [7], (iii) high impedance

* Corresponding author: Nikolay Atanasov (natanasov@windowslive.com).
[1] Research Center for Advanced Materials Science (RCAMS), King Khalid University, Abha 61413, P. O. Box 9004, Saudi Arabia.
[2] Department of Chemistry, College of Science, King Khalid University, Abha 61413, P. O. Box 9004, Saudi Arabia. [3] Department of Physics, Faculty of Science, King Abdulaziz University, Jeddah, Saudi Arabia. [4] Department of Polymer Engineering, University of Chemical Technology and Metallurgy, 1756 Sofia, Bulgaria. [5] Department of Telecommunications, Faculty of Telecommunications and Management, University of Telecommunications and Post, 1700 Sofia, Bulgaria. [6] Department of Communication and Computer Engineering, Faculty of Engineering, South-West University 'Neofit Rilski', 2400 Blagoevgrad, Bulgaria.

surfaces (HIS) [8] or (iv) antenna with full ground plane [9]. The presence of the metasurface or full ground plane improves antenna performance while decreasing backside radiation. An alternate approach is to improve antenna performance while decreasing backside radiation through dipole structures combined with a reflector. The latter approach has been used in this paper.

In order to make the antenna flexible, alternative materials to replace existing substrates that are rigid have been considered [10]. Bendable materials such as polydimethylsiloxane, conductive fabrics, liquid metal alloys, polymers in paper and rubber composites are widely used in current designs of flexible electronic devices [11]. Among available materials, rubber composites are attractive because they exhibit a good balance of mechanical and electromagnetic properties over a wide frequency range. The low production cost and ease of manufacturing are also added advantages for rubber.

In this paper, we propose and experimentally demonstrate a flexible planar dipole antenna on rubber composite integrated with a reflector. The proposed design offers several advantageous characteristics, such as good impedance matching and bandwidth, high antenna efficiency in vicinity of the human body, low SAR level over the frequency band of 2.40–2.50 GHz, and more importantly, low fabrication cost and complexity.

2. PREPARATION AND CHARACTERIZATION OF RUBBER COMPOSITES

In this paper, nitrile butadiene rubber (NBR) polymer composite is chosen as the antenna's multilayer composite due to its good balance of physical, chemical and electromagnetic properties over a wide frequency range. The composition of the NBR multilayer composite in phr (parts in wt per 100 parts in wt of dry rubber) is as follows: nitrile butadiene rubber (100.0 phr), zinc oxide (3.0 phr), stearic acid (1.0 phr), processing oil (10.0 phr), isopropyl-phenyl-p-phenylenediamine (1.0 phr), N-tert-Butyl-2-benzothiazolesulfenamide (0.7 phr), and sulphur (1.5 phr). The elastomer compounds were prepared in an open laboratory two rolls mill with rolls dimensions L/D 320 mm × 160 mm and 1.27 friction. The speed of the slow roll was $25\,min^{-1}$. Test samples were vulcanized to plates with dimensions 150 mm × 150 mm in vulcanization optimum, determined according to their vulcanization isotherms (ISO 3417:2010) at 160°C in an electrically heated vulcanization hydraulic press at 10 MPa using a steel press form.

Designing rubber-based antennas requires knowledge of the dielectric properties of the substrates at the intended frequency of use [11]. In this paper, the electromagnetic parameters of the proposed material are measured by the resonant perturbation method described in [12]. The tested sample was introduced into a rectangular cavity resonator, placed at the position of maximum intensity of electric field, and the electromagnetic parameters of the sample were deduced from the change in the resonant frequency and quality factor of the resonator. The real part of the relative permittivity (ε_r') is 2.9312, and imaginary part (ε_r'') is 0.1050 at frequency 3.1287 GHz. Measured values of ε_r' and ε_r'' were used to determine the conductivity and tangent of the dielectric loss angle ($\tan\delta_\varepsilon$) of the composite sample. The effective conductivity of the composite is 0.0183 S/m and $\tan\delta_\varepsilon$ is 0.035.

3. ANTENNA DESIGN AND PARAMETRIC STUDY

3.1. Antenna Design

Design configuration of the proposed antenna is illustrated in Figure 1. It consists of a modified version of the planar dipole antenna composed of one dipole arm and a microstrip line placed on the top side of the rubber composite substrate (Layer 1) whereas the second arm and a small rectangular ground plane are placed on the other side. Considering that wearable antennas operate in close proximity to the human body, a metal rectangular reflector (width 40 mm and length 50 mm) is added, for isolates the antenna from the effects of human tissue loading. The reflector is sandwiched between two 1.85 mm thick NBR composite layers (Layers 2 and 3). This topology is chosen due to its simplicity and because planar monopole and dipole antennas have received more attention over other antenna types especially in wearable and flexible applications [13].

In order to minimize the antenna size, we replace the large rectangular dipole arms by two shortened with capacitor metal plates attached to their ends as shown in Figure 1. To achieve the desired optimal
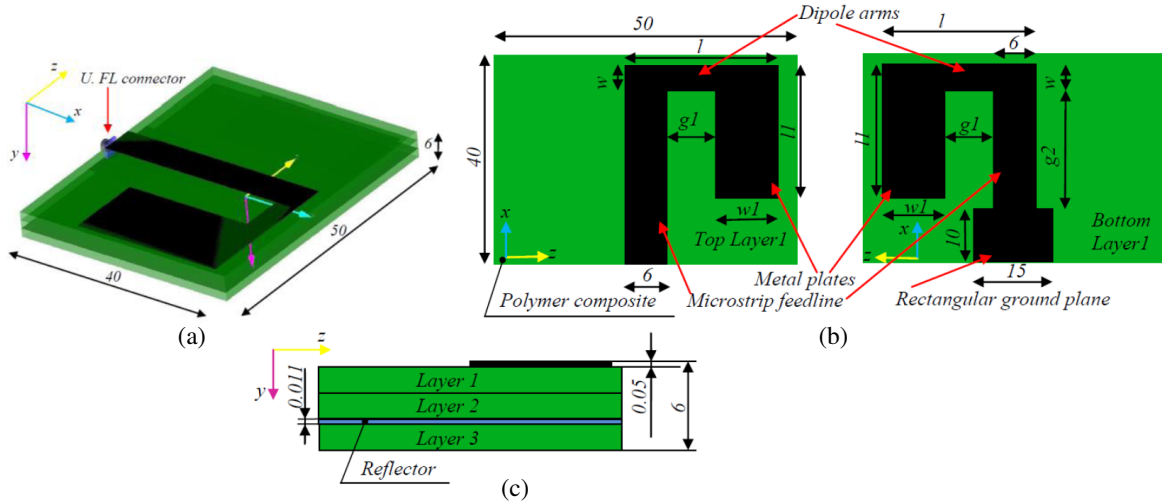
Figure 1. Configuration of the flexible planar dipole antenna on multilayer rubber composite integrated with a reflector: (a) 3D model with U. FL RF connector, (b) top and bottom views of the antenna top structure on the first composite layer (Layer 1), (c) cross sectional view in yz-plane.

radiation efficiency at low SAR level in human tissue, the geometrical dimensions of antenna were tuned in the presence of human body model. A three-layer human body model was employed, consisting of skin, fat, and muscle tissue layers. The thickness and electromagnetic properties of the layers considered in the body model [14] are tabulated in Table 1. The electromagnetic parameters of the tissues were assumed as in [15] at frequency 2.45 GHz. The overall surface size of the model is: $120 \, \text{mm} \times 120 \, \text{mm}$.

Table 1. Material properties of three-layer human tissue model.

	Relative permittivity	Conductivity (S/m)	Density (kg/m^3)	Thickness (mm)
Skin	38.007	1.464	1020	1
Fat	5.280	0.105	918	6
Muscle	53.574	1.810	1040	50

Design and analysis of the antenna are carried out using the full wave electromagnetic simulation software XFDTD (XFDTD, Remcom Inc., State College, PA, USA) which is based on the finite-difference time-domain (FDTD) method. The nonuniform mesh technique is used to calculate the SAR and input characteristics of the antenna. In this work, 0.5 mm fine-size cells are used around the antenna and up to 20 cells in space around it. The rest of problem space is modelled by the coarse-size cells of 1 mm.

3.2. Parametric Study

In order to optimize the antenna design, the proposed antenna is investigated for variation of design parameters. The parametric study of the antenna has been carried out by changing only one dimension at a time when the antenna is placed directly over the skin of body model. In this paper, only radiation efficiency, SAR, and input impedance stability in presence of human body model are employed as criteria for optimization.

3.2.1. Dipole Capacitor Metal Plates Width Variation (w1)

The width of dipole capacitor metal plates is varied to thirteen ($w1$ is varied from 0.5 mm to 12.0 mm). The input impedance (Zin), voltage standing wave ratio (VSWR), radiation efficiency, maximum gain

and SAR values of the proposed antenna are analyzed.

Figure 2(a) shows the input impedance and VSWR of the proposed dipole antenna with respect to the capacitor plate width $w1$. We can observe that the variation of the input impedance against the capacitor plate width is small, and the input impedance is well matched to the load 50 ohms when $w1$ is between 0.5 mm and 8 mm. The input impedance at resonant frequency decreases with increase in dipole capacitor plate width.

Simulated radiation efficiency and maximum gain graphs as a function of the capacitor element width are depicted in Figure 2(b). These graphs show that both radiation efficiency and maximum gain increase when the width of capacitor plates is increased, which occurs because larger plate surface increases the area that the current can flow over. It is known that the radiation power of the antenna is proportional to the multiple of the radiation resistance and the square of the current [16]. However, the resonant frequency is monotonically shifted to higher values when the width of capacitor plates is increased due to the decrease in electrical length ($g1$ decrease).

Figure 2(d) shows the SAR values in the human body model as a function of the capacitor plate width. It is found that SAR values vary with respect to the capacitor plate width $w1$. The maximum 1 g and 10 g average SAR values are minimized when the capacitor plate width $w1$ becomes 3 mm. Then the maximum 1 g and 10 g average SAR values are insignificantly increased with increase in dipole capacitor plate width.
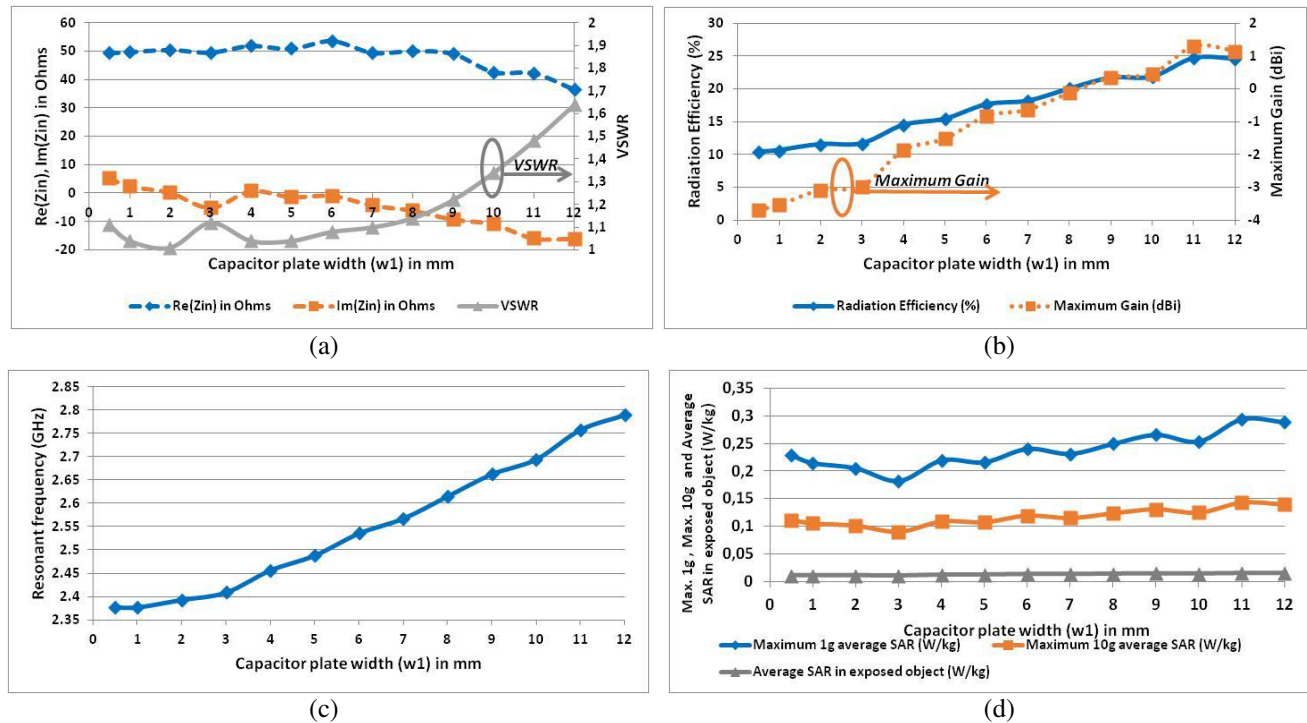
Figure 2. Plot of (a) input impedance and VSWR, (b) radiation efficiency and maximum gain, (c) resonant frequency, (d) SAR of proposed antenna placed directly over the skin of body model versus capacitor metal plate width ($w1$).

3.2.2. Dipole Arm Width Variation (w)

The input impedance plot and VSWR for four values of dipole width ($w = 1$, 2, 3 and 6 mm) are shown in Figure 3(a). We can observe that the real part of input impedance takes a value of 50 ohms at $w = 2$ mm. However, when w becomes larger than 3 mm, the resistance and reactance traces move from the area of the optimal impedance, and as a consequence, the VSWR rises up to 1.64. However, we must point out that both radiation efficiency and maximum gain increase when dipole width is increased
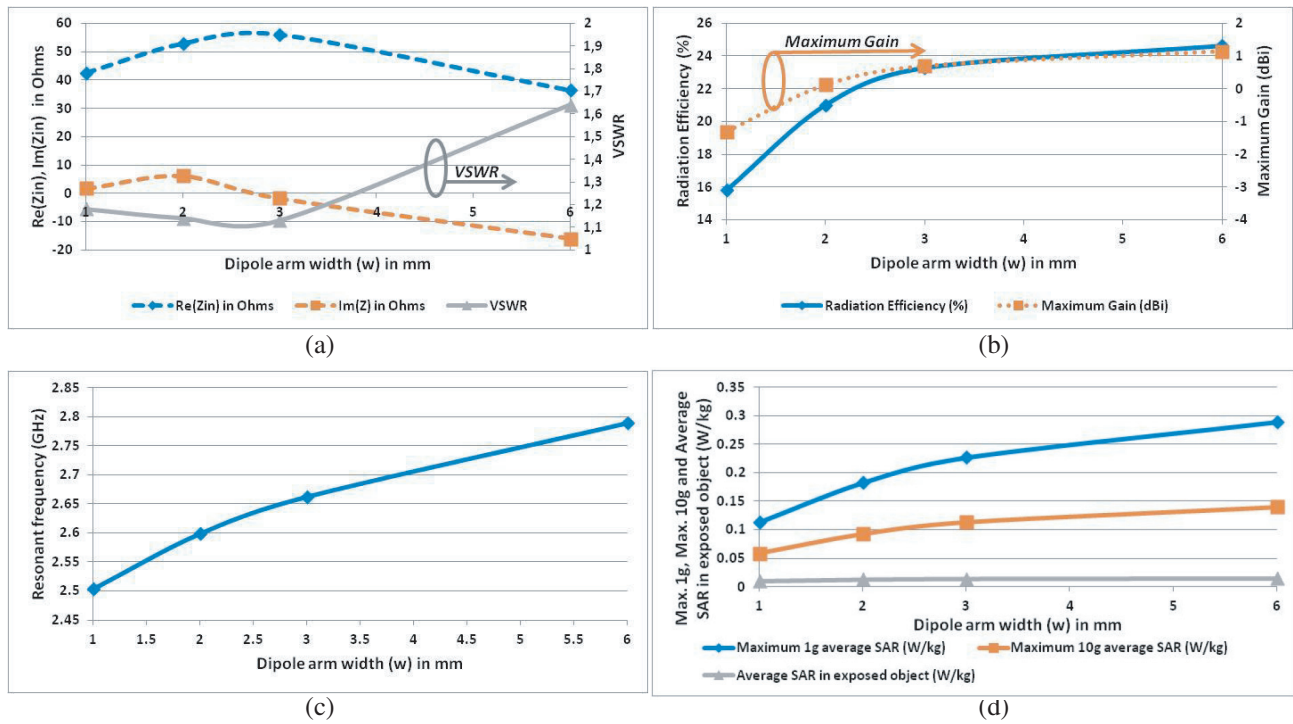
Figure 3. Plot of (a) input impedance and VSWR, (b) radiation efficiency and maximum gain, (c) resonant frequency, (d) SAR of proposed antenna placed directly over the skin of body model versus dipole arm width (w).

which occurs because larger dipole arms increase the area that the current can flow over. Results in Figure 3(c) also indicate that the resonant frequency is monotonically shifted to higher values with increase in w. Finally, it should be noted that maximum 1 g and 10 g average SAR values are shifted to higher values with increase in the dipole width.

3.2.3. Dipole Capacitor Metal Plates Length Variation (l1)

The length of dipole capacitor plates is varied to four values ($l1 = 24$, 25, 26, and 27 mm). As can be seen in Figures 4(a) and (c), the real part of the input impedance is increased due to increase in the length of dipole capacitor plates, while resonant frequency is decreased. Moreover, the radiation efficiency varies from 18.94% ($l1 = 24$ mm) to 19.07% ($l1 = 26$ mm) then down to 17.23% ($l1 = 27$ mm) as shown in Figure 4(b). Results shown in Figure 4(d) also indicate small variations in the 1 g and 10 g average SAR values.
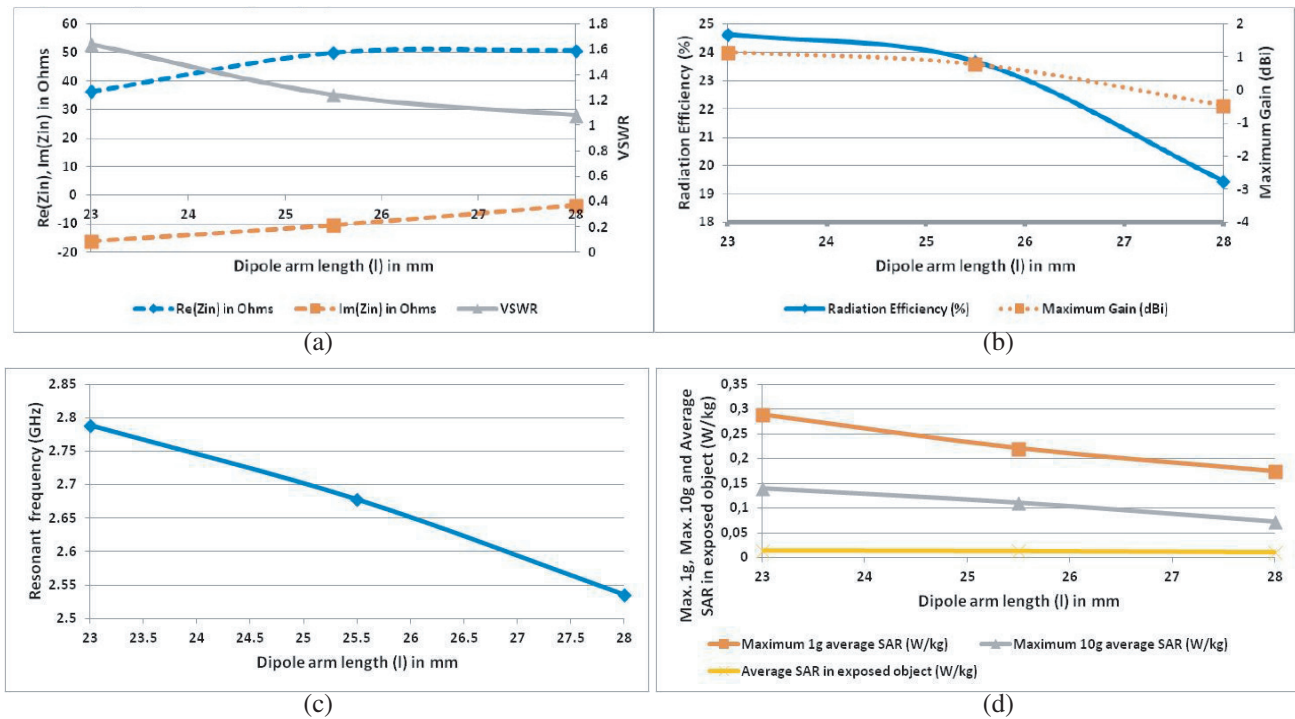
3.2.4. Dipole Arm Length Variation (l)

Figure 5(a) shows the simulated input impedance and VSWR of the antenna vs dipole arm length. The length of dipole arm is varied to three values ($l = 23.0$, 25.5, and 28.0 mm). We can observe that the real part of input impedance takes a value of 50 ohms at $l = 25.5$ mm. Results in Figures 5(b)–(d) indicate two main effects due to dipole arm length increase: one is that both radiation efficiency and maximum gain decrease; the other is that the maximum 1 g and 10 g average SAR values are minimized to 0.22 and 0.11 W/kg, respectively when the dipole arm length becomes 28 mm.

We conclude that parameters w and $w1$ are very important factors to obtain both high radiation efficiency and maximum gain. To increase antenna efficiency, the size of the radiating elements has to be increased. The results discussed above also indicate that the resonant frequency can be controlled effectively and tuned by adjusting the dimensions w, $w1$, l, and $l1$.

(a)

(b)

(c)

(d)
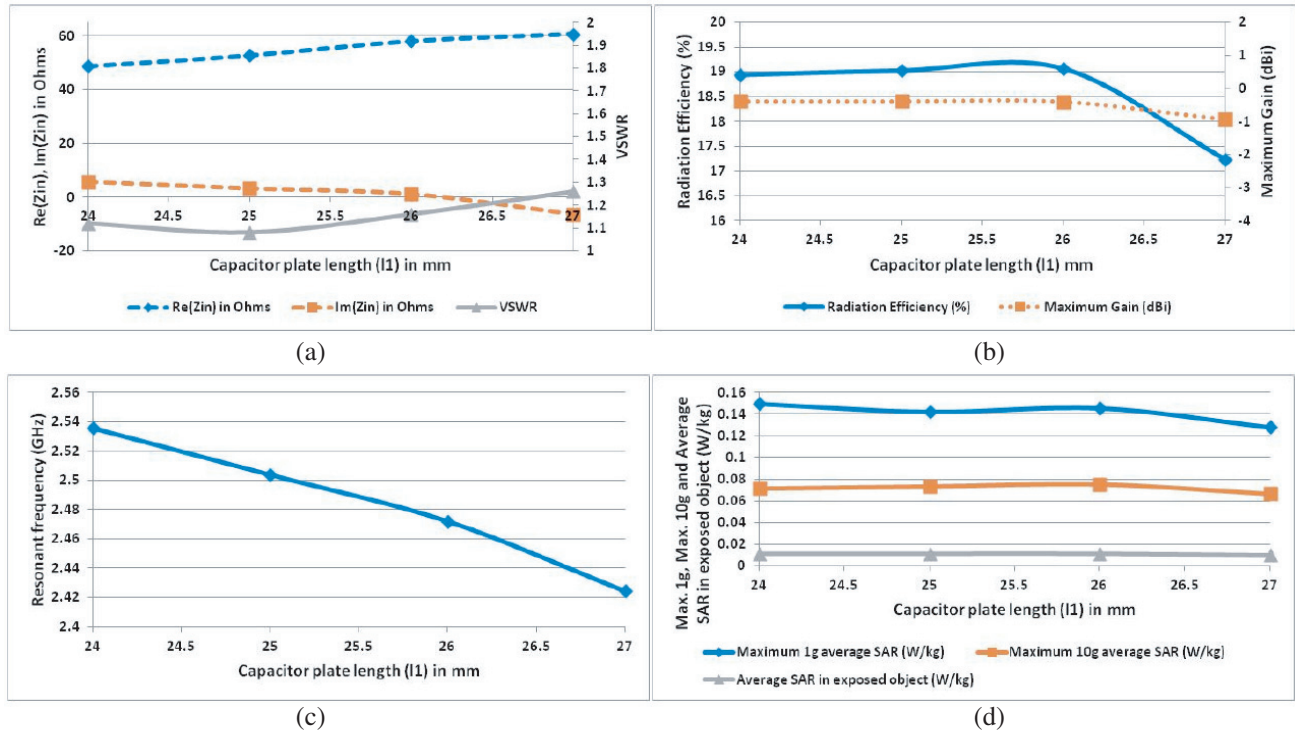
Figure 4. Plot of (a) input impedance and VSWR, (b) radiation efficiency and maximum gain, (c) resonant frequency, (d) SAR of proposed antenna placed directly over the skin of body model versus capacitor pates length ($l1$).

(a)

(b)

(c)

(d)

Figure 5. Plot of (a) input impedance and VSWR, (b) radiation efficiency and maximum gain, (c) resonant frequency, (d) SAR of proposed antenna placed directly over the skin of body model versus dipole arm length (l).

To make a compromise among the efficiency, matching and size, we chose $w1 = 13.5\,\text{mm}$ and then adjust $w = 3\,\text{mm}$, $l = 27\,\text{mm}$ and $l1 = 27\,\text{mm}$ to make the antenna operate at the center frequency of $2.44\,\text{GHz}$ (in free space) and $2.45\,\text{GHz}$ when the antenna is placed on the skin of human body phantom.

4. ANTENNA FABRICATION AND RESULTS

The final optimized design is fabricated (components of proposed antenna were fabricated separately and assembled with glue). A U. FL connector was soldered to the stripline feed and ground plane. Photographs of the fabricated antenna are shown in Figures 6 and 7.

The wearable antenna characteristics are influenced mainly by the electromagnetic properties of the human tissues. Therefore, an analysis of antenna characteristics as a function of body proximity is necessary. In order to experimentally evaluate the performance of the proposed antenna on human body, appropriate tissue-equivalent phantom was developed. Tissue-equivalent phantom with dimensions $100\,\text{mm}$ (x), $47\,\text{mm}$ (y) and $117\,\text{mm}$ (z) to emulate muscle tissue was designed and fabricated accordingly to the recipe and technique described in [17]. After the phantom mixtures had solidified, electromagnetic properties measurements were carried out by the resonant perturbation method. The real part of the relative permittivity is 41.17, and conductivity is $2.91\,\text{S/m}$ at $3.1287\,\text{GHz}$. The fabricated phantom with antenna prototype is illustrated in Figure 6(a). Moreover, a numerical homogeneous model consists only of muscle tissue with electromagnetic parameters pointed above (relative permittivity 41.17 and conductivity $2.91\,\text{S/m}$) was developed (Figure 6(b)). The total size of the homogeneous

(a)   (b)

Figure 6. (a) Photograph of the fabricated tissue-equivalent phantom with antenna prototype, (b) numerical model of proposed antenna placed on homogeneous tissue-equivalent model.
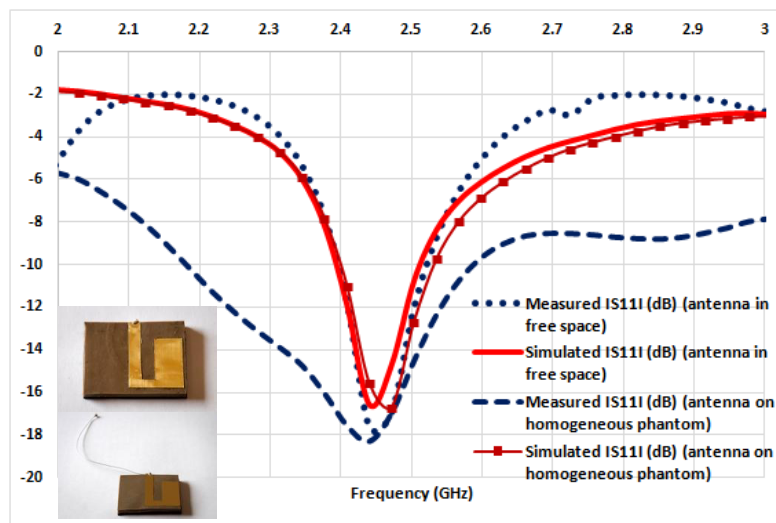

Figure 7. Measured and simulated reflection coefficient magnitude as a function of the frequency of the proposed antenna in free space, on fabricated tissue-equivalent phantom and on homogeneous numerical model and photographs of the proposed antenna with U. FL RF connector and coaxial cable.

model is 100 mm (x), 47 mm (y) and 117 mm (z). Comparisons between results for performance of the antenna on numerical homogeneous tissue model and fabricated tissue-equivalent phantom in terms of $|S_{11}|$, radiation pattern, bandwidth and SAR are listed below.

The measured and simulated reflection coefficient magnitudes of the proposed antenna in free space, on fabricated phantom and on homogeneous numerical model are shown in Figure 7. The antenna's S-parameters were measured using an Agilent FieldFox Network Analyser. Good agreement between measurement and simulation is achieved. The measured resonant frequency in free space is 2.454 GHz compared to 2.440 GHz predicted by simulation (a 0.6% difference). The measured reflection coefficient magnitude of the proposed antenna on fabricated phantom is -18.31 dB at 2.44 GHz, while the simulated reflection coefficient magnitude is -16.68 dB at 2.47 GHz. Both of the measured and simulated results show that the antenna has VSWR < 2 bandwidth from 2.395 GHz to 2.521 GHz in free space and from 2.395 GHz to 2.530 GHz on homogeneous tissue-equivalent phantom. The proposed antenna sufficiently covers the industrial, scientific and medical band.

Next, the radiation characteristics in free space and on tissue-equivalent phantom were measured. The simulated and measured normalized radiation patterns of the proposed antenna in free space, on tissue-equivalent phantom and on numerical homogeneous phantom are shown in Figure 8. As shown in Figure 8, the measured radiation patterns in xy-plane and yz-plane agree well with the simulated results, confirming the predicted behavior of the proposed antenna design.
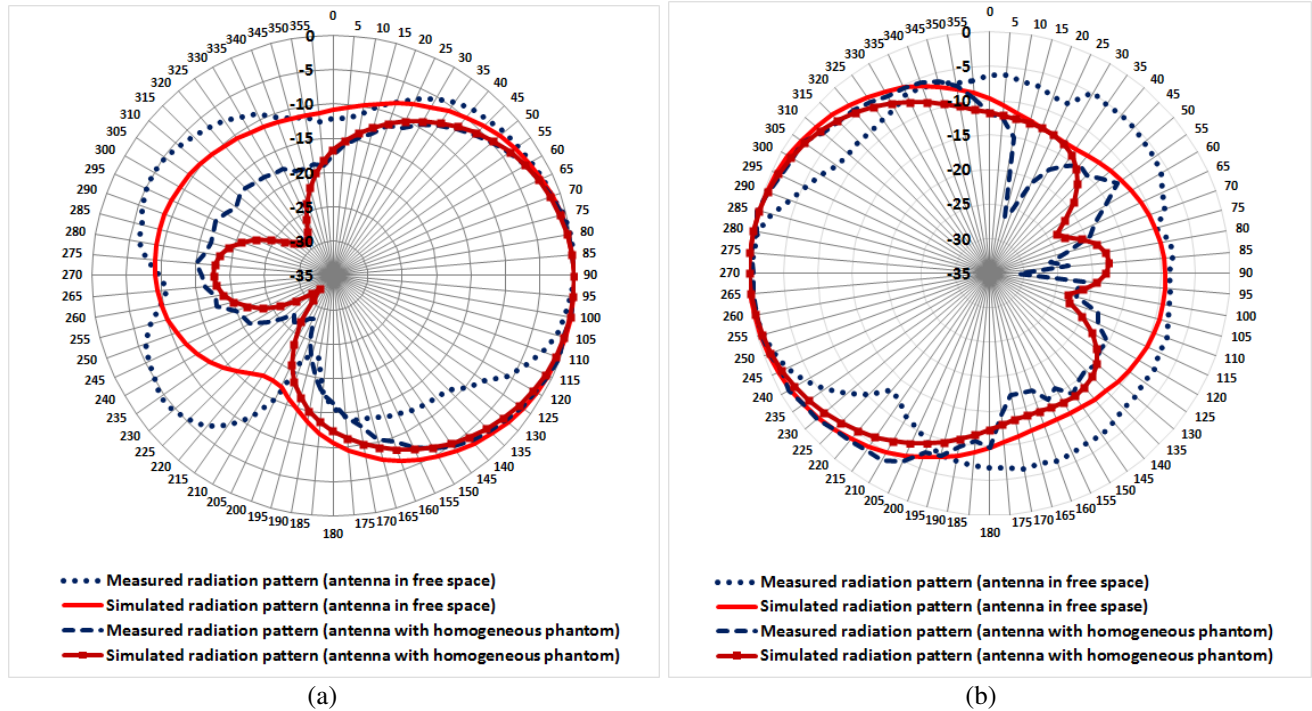

Figure 8. Simulated and measured normalized radiation pattern for proposed antenna in free space, on fabricated tissue-equivalent phantom and on homogeneous numerical model (a) in xy-plane, (b) in yz-plane.

The impact of a wearable antenna on human tissue, characterized by the specific absorption rate, also was investigated. The SAR spatial distribution in numerical (homogeneous and three-layer) human body models was computed using a FDTD numerical technique. The 12-field components approach was used to calculate SAR in the voxel. All results were normalized to net input power level 100 mW.

Figure 9 shows 1 g average SAR values in three-layer human body model when the proposed antenna is placed on the skin of body model. It can be observed that the peak 1 g average SAR value is less than 0.23 W/kg, well below the European and American standards (2 W/kg and 1.6 W/kg). In the figure, we observe that maximum 1 g average SAR (0.23 W/kg per 100 mW of antenna delivered power)
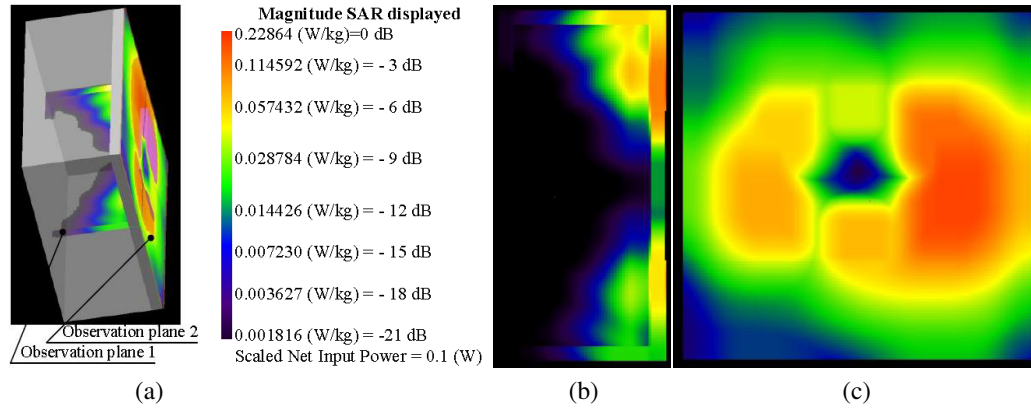
Figure 9. SAR distributions in three-layer human body model when proposed antenna is placed on skin of body model, (a) observation planes, (b) SAR distributions for observation plane 1, (c) SAR distributions for observation plane 2.
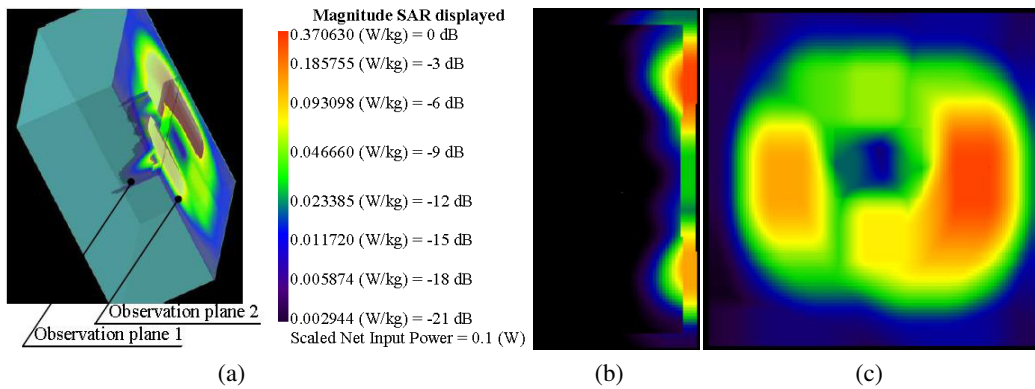
Figure 10. SAR distributions in homogeneous human body model when proposed antenna is placed on the surface of body model, (a) observation planes, (b) SAR distribution for observation plane 1, (c) SAR distribution for observation plane 2.

occurs at the skin layer near the antenna edge, and most power absorption is localized near the skin. It is important to note that the SAR values at the skin layer underneath the antenna are considerably reduced (from 0.028 to 0.002 W/kg). This occurs because the reflector and Layer 3 of polymer composite lie between the antenna and the human body model, providing some degree of shielding from exposure.

Figure 10 presents the distribution of 1 g average SAR values in homogeneous human body model when the proposed antenna is placed on the surface of body model. As can be seen, near the surface of the homogeneous model, the 1 g average SAR with the homogeneous model is larger than that with the three-layer body model. The reason for this high SAR results may be from the higher conductivity of the homogeneous model.

5. COMPARATIVE STUDY

To demonstrate the advantages of the flexible planar dipole antenna on multilayer rubber composite with reflector, performance of the proposed antenna was compared to a half wave dipole antenna. The dimensions of the half wave dipole are based on the reference dipole for 2.45 GHz, described in IEEE Standard 1528 [18]. The numerical antenna model was modeled as a perfect electrical conductor and fed symmetrically at the center.

Bandwidth at reflection coefficient magnitude lower than -10 dB and the resonant frequency of

the reference dipole and proposed antenna in free space and in the presence of three-layer human body model are listed in Table 2. The radiation efficiency, maximum realized gain and SAR values are also listed in the table.

Two main observations can be made from the results of Table 2. First, when the reference dipole is placed on the skin of the human body model, the resonant frequency is sifted down by 1.309 GHz, attributed to the difference in the capacitive loading between the near field and dipole antenna. Second, the presence of the human body model near the antenna could bring different results in the bandwidth. For half wave dipole antenna, a wider bandwidth was observed when the antenna was placed on the skin. For the proposed antenna, the results indicate that resonant frequency and bandwidth are almost the same when operating in free space and close to the human body model.

Table 2. Comparison of half wave dipole antenna with the proposed antenna.

	Resonant frequency (GHz)	BW^a (MHz)	Rad. Eff.^{b} (%)	Max. Gain^c (dBi)	Max. 1 g average SAR (W/kg)
Proposed antenna in free space	2.4404	126.78	23.2	−0.292	-
Proposed antenna on three-layer body model	2.4720	145.43	20.5	−0.075	0.228
Proposed antenna at distance 10 mm from three-layer body model	2.4562	119.58	16.84	−1.412	0.121
Half wave dipole in free space	2.5671	380.32	100	2.164	-
Half wave dipole on three-layer body model	1.1409	1489.60	1.98	−13.04	14.557
Half wave dipole at distance 10 mm from three-layer body model	2.6622	538.78	20.61	0.497	2.420

^{a}BW = Bandwidth. ^{b}Rad. Eff. = Radiation Efficiency. ^{c}Max. Gain = Maximum Gain.

Moreover, the radiation efficiency of half wave dipole decreases drastically from 100% in free space to 1.98% on the skin of tissue model while the efficiency of the proposed antenna remains stable when it is positioned at various distances from human body model. From Table 2, we see that the proposed antenna efficiency varies from 23.2% in free space to 20.5% on the skin of the human tissue model. This demonstrates that the rectangular reflector and the third layer of NBR polymer composite isolate the antenna well from the body and prove the effectiveness of the proposed antenna in providing a better communication link and lower coupling with the user's body.

From the results reported in Table 2 it can be noted that there is a significant difference between the maximum SAR in human body model caused by the reference dipole and those caused by the proposed antenna. In Table 2 we see that for the 100 mW input power, the half wave dipole generates a maximum 1 g average SAR value about 14.557 W/kg due to its omnidirectional radiation characteristic. Even at a distance of 10 mm away from the body model, the half wave dipole produces a maximum 1 g average SAR value of 2.420 W/kg. In contrast, with the proposed antenna, the maximum 1 g average SAR value drops to 0.229 W/kg when the antenna is placed on the skin of body model. In other words,

the proposed antenna reduces the 1 g average SAR by more than 95%, demonstrating the superiority of the proposed antenna for operation in close proximity to the human body.

Finally, comparisons between the proposed wearable antenna and those previously published in terms of SAR, radiation efficiency, bandwidth, dimensions and resonant frequency are listed in Table 3. As a result, one can say that the proposed antenna has lower 1 g average SAR value than the antennas in [5, 6, 8, 9], and smaller dimensions than those in [5, 6]. Moreover, the proposed antenna has a broader bandwidth than antennas in [5, 6, 9] and better radiation efficiency than [19] when it is mounted directly on a human tissue model as a wearable antenna for body-centric communications. Other advantages of the proposed antenna are the low cost and simple fabrication process.

Table 3. Comparison of different flexible antennas with the proposed antenna.

References and proposed antenna	Max. 1 g average SAR* (W/kg)	Rad. Eff. (%) on body	BW (MHz) on body	Dimensions (mm)	Resonant frequency (GHz)
Proposed antenna	0.1	20.5	145	$50 \times 40 \times 6$	2.44
[5] integrated planar antenna	0.67	NA	130	$62 \times 42 \times 4.5$	2.40
[6] antenna with EBG	0.16	NA	125	$124 \times 90 \times 1$	2.45
[8] integrated antenna on HIS	0.29	38	150	$38 \times 38 \times 3$	2.50
[9] antenna with full ground plane	0.61	NA	60	$14 \times 80 \times 1.6$	2.45
[19] antenna with parasitic element	NA	20	NA	$50 \times 30 \times 5.5$	2.45

Max. 1 g average SAR*- Maximum 1 g average SAR value at a distance 2 mm away from the human tissue model. All results were normalized to net input power level 100 mW; NA — not available.

6. CONCLUSION

In this paper, the design, fabrication, and testing of a flexible and compact planar dipole antenna on multilayer rubber composite are discussed in details. The antenna is analyzed for various design parameters to optimize the design for high radiation efficiency and low SAR level in human tissue. The antenna achieves more than 20% on-body radiation efficiency, and the peak 1 g average SAR value is less than 0.23 W/kg when the antenna is placed directly over the skin of body model. Based on the measured results and the advantages possible for SAR reduction, the proposed planar dipole antenna on rubber substrate offers a good solution for wearable applications.

ACKNOWLEDGMENT

REFERENCES

1. Chen, J. W. and H. Mitomo, "The underlying factors of the perceived usefulness of using smart wearable devices for disaster applications," *Telematics and Informatics*, Vol. 34, 528–539, 2017.

2. Yang, H., W. Yao, Y. Yi, X. Huang, S. Wu, and B. Xiao, "A dual-band low-profile metasurface-eanabled wearable antenna for WLAN devices," *Progress In Electromagnetic Research*, Vol. 61, 115–125, 2016.

3. Genovesi, S., F. Costa, F. Fanciulli, and A. Monorchio, "Wearable inkjet-printed wideband antenna by using miniaturized AMC for sub-GHz applications," *IEEE Antennas and Wirelesss Propagation Letter*, Vol. 15, 4027–4030, 2016.

4. Al-Ghamdi, A., O. Al-Hartomy, F. Al-Solamy, N. Dishovsky, N. Atanasov, and G. Atanasova, "Enhancing antenna performance and SAR reduction by a conductive composite loaded with carbon-silica hybrid filler," *International Journal of Electronics and Communications (AEÜ)* Vol. 70, 668–675, 2017.

5. Jiang, Z., D. Brocker, P. Sieber, and D. Werner, "A compact, low-profile metasurface-enabled antenna for wearable medical body-area network devices," *IEEE Trans. Antennas Propag.*, Vol. 62, 4021–4030, 2014.

6. Velan, S., E. Florence, M. Kanagasabai, A. Sarma, C. Reviteja, R. Sivasamy, and J. Pakkathillam, "Dual-band EBG integrated monopole antenna deploying fractal geometry for wearable applications," *Antennas Wireless Propag. Lett.*, Vol. 14, 249–252, 2015.

7. Raad, H., A. Abbosh, H. Al-Rizzo, and D. Rucker, "Flexible and compact AMC based antenna for telemedicine applications," *Antennas Wireless Propag. Lett.*, Vol. 61, 524–531, 2013.

8. Chen, Y. and T. Ku, "A low-profile wearable antenna using a miniature high impedance surface for smart watch applications," *Antennas Wireless Propag. Lett.*, Vol. 15, 1144–1147, 2016.

9. Abbas, S. M., K. Esselle, and Y. Ranga, "A printed antenna with a ground plane and electromagnetically coupled feed for 2.45 GHz body area networks," *APSURSI, IEEE*, 2143–2144, 2013.

10. Affendi, N. A. M., N. A. L. Alias, N. M. Razali, Z. Awang, and A. Samsuri, "Flexible antennas using a new material," *Proceedings of Asia-Pacific Microwave Conference*, 1420–1422, 2014.

11. Zaiki, A., N. A. M. Affendi, N. A. L. Alias, and N. M. Razali, "Flexible antennas based on natural rubber," *Progress In Electromagnetic Research*, Vol. 61, 75–90, 2016.

12. Chen, L. F, C. K. Ong, C. Neo, V. V. Varadan, and V. K. Varadan, *Microwave Electronics: Measurement and Materials Characterization*, 1st Edition, John Wiley & Sons, Ltd., Chichester, 2004.

13. Raad, H. K., H. M. Al-Rizzo, A. Issac, and A. I. Hammoodi, "A compact dual band polyimide based antenna for wearable and flexible telemedicine devices," *Progress In Electromagnetics Research C*, Vol. 63, 153–161, 2016.

14. Hu, B., G.-Gao, L.-L. He, X.-D. Cong, and J.-N. Zhao, "Bending and on-arm effects on a wearable antenna for 2.45 GHz body area network," *IEEE Antennas Wireless Propag. Lett.*, Vol. 15, 378–381, 2015.

15. https://www.fcc.gov/general/body-tissue-dielectric-parameters.

16. Fujimoto, K., "Antennas for mobile communications," C. A. Balanis editor, *Modern Antenna Handbook*, 1143–1228, Hoboken, John Wiley & Sons, Inc., 2008.

17. Yialmaz, T., R. Foster, and Y. Hao, "Broadband tissue mimicking phantoms and a patch resonator for evaluation noninvasive monitoring of blood glucose levels," *IEEE Trans. Antennas Propag.*, Vol. 62, 3065–3075, 2014.

18. IEEE for Recommended Practice for Determining the Peak Spatial-Average Specific Absorption Rate (SAR) in the Human Head from Wireless Communications Devices: Measurement Techniques, IEEE Standard 1528, 2003.

19. Varnoosfaderani, M. V., D. V. Thiel, and J. Lu, "External parasitic elements on clothing for improved performance of wearable antennas," *IEEE Sensors Journal*, Vol. 15, No. 1, 307–315, 2015.